Contents lists available at ScienceDirect

Regenerative Therapy

journal homepage: http://www.elsevier.com/locate/reth

Original Article

Development of chimeric antigen receptor T cells targeting cancer-expressing podocalyxin

Yuta Mishima [a, b, 1], Shintaro Okada [c, 1], Akihiro Ishikawa [c], Bo Wang [c],
Masazumi Waseda [c], Mika K. Kaneko [d], Yukinari Kato [d], Shin Kaneko [a, b, c, *]

[a] Department of Cancer Immunotherapy and Immunology, Institute of Medicine, University of Tsukuba, Tsukuba, Ibaraki 305-8575, Japan
[b] Division of Cancer Immunotherapy, Transborder Medical Research Center, University of Tsukuba, Tsukuba, Ibaraki 305-8577, Japan
[c] Department of Cell Growth and Differentiation, Center for iPS Cell Research and Application (CiRA), Kyoto University, Kyoto 606-8507, Japan
[d] Department of Antibody Drug Development, Tohoku University Graduate School of Medicine, Sendai, Miyagi 980-8575, Japan

ABSTRACT

Chimeric Antigen Receptor (CAR)-T cell therapy has revolutionized the treatment of CD19-positive B-cell malignancies. However, the field is rapidly evolving to target other antigens, such as podocalyxin (PODXL), a transmembrane protein implicated in tumor progression and poor prognosis in various cancers. This study explores the potential of PODXL-targeted CAR-T cells, utilizing a cancer-specific monoclonal antibody (CasMab) technique to enhance the specificity and safety of CAR-T cell therapy. We developed CAR-T cells based on the single-chain variable fragment (scFv) derived from the cancer-specific monoclonal antibody PcMab-6, which selectively targets glycosylation modifications on PODXL-expressing cancer cells. As a control, CAR-T cells were also generated from PcMab-47, a non-cancer-specific antibody for PODXL. *In vitro* experiments demonstrated that CAR-T cells based on PcMab-6 exhibited significant antitumor activity with reduced off-target effects on normal cells compared to PcMab-47-derived CAR-T cells. Additionally, to enhance the persistence and therapeutic efficacy of these CAR-T cells, we developed a humanized version of PcMab-6 scFv. The humanized CAR-T cells showed extended antitumor effects *in vivo*, demonstrating the potential for prolonged therapeutic activity. These findings underscore the utility of CasMab technology in generating highly specific and safer CAR-T cell therapies for solid tumors, highlighting the promise of humanized CAR-T cells for clinical application.

1. Introduction

Chimeric antigen receptors (CARs) are artificially engineered receptors that possess a single-chain variable fragment (scFv) derived from monoclonal antibodies in their extracellular domain and either CD3z or CD3z in combination with costimulatory molecules in their intracellular domain [1,2]. The first CAR-T cell product targeting CD19-positive B-cell malignancies demonstrated a remarkable therapeutic effect by extending patient survival. The current research landscape is shifting towards developing CAR-T cells recognizing antigens other than CD19. This study's unique contribution lies in exploring podocalyxin (PODXL) as a potential target for CAR-T cell therapy. PODXL is a type I transmembrane protein with a molecular weight of 150,000—200,000, characterized by highly N- or O-linked glycosylation [3—5]. Known as TRA-1-60 and TRA-1-81 antigens, PODXL is recognized as a pluripotent stem cell marker [4,6—9]. PODXL is expressed in tissues such as the kidney, heart, pancreas, and breast, playing critical roles in developing certain tissues [10]. Moreover, PODXL has been implicated in promoting tumor growth, invasion, and metastasis [11,12], serving as a diagnostic marker and prognostic indicator for certain cancers such as brain tumors [5], colorectal cancer [13], renal cancer [14], and oral cancer [15]. Consequently, high PODXL expression could

negatively impact overall survival (OS), disease-specific survival (DSS), and disease-free survival (DFS) in several cancers.

Previously, the mouse monoclonal antibody PcMab-47 was developed by immunizing mice with recombinant soluble PODXL purified from the supernatant of LN229/ectodomain-PODXL cells [16]. Although PcMab-47 is highly effective in detecting PODXL immunohistochemically, it reacts not only with cancer cells but also with normal cells such as vascular endothelial cells [17–20], potentially causing severe side effects, thus precluding clinical application. Hence, cancer-specificity is essential to mitigate side effects on normal tissues in antibody therapies targeting PODXL-expressing cancers.

Addressing the challenge of cancer-specificity, the cancer-specific monoclonal antibody (CasMab) technique was developed [21]. CasMab can recognize aberrantly glycosylated proteins specific to cancer cells [21]. The monoclonal antibody PcMab-6 was further developed, specifically targeting PODXL on cancer cells. This study generated CAR-T cells from the scFv region of PcMab-6 and PcMab-47, which was used as a control. The results demonstrated the antitumor effect of these CAR-T cells on solid tumors *in vitro* and *in vivo* animal models. Furthermore, compared to CAR-T cells generated from PcMab-47, CAR-T cells generated from PcMab-6 showed reduced reactivity towards PODXL-expressing normal cells. These results underscored CasMab technology's potential in enhancing CAR-T cell therapy's safety and specificity.

Recently, it has been reported that extending the duration of CAR-T cells in patients can improve therapeutic efficacy. One approach to prolong CAR-T cell persistence is to use a humanized version of the animal-derived scFv sequence of the CAR. Clinical trials have demonstrated that modified CD19 CAR-T cells exhibit higher therapeutic effectiveness compared to the original CD19 CAR-T cells [22]. As such, we developed humanized CAR-T cells carrying the human-scFv (h_) sequence, which is a humanized version of the mouse-derived scFv (m_) sequence of PcMab-6 [23]. We then evaluated the anti-tumor effect of CAR-T cells in an *in vivo* animal model against solid tumors. The results revealed an extended anti-tumor effect of humanized CAR-T cells.

2. Material and methods

2.1. Cell lines and peripheral blood mononuclear cells

To prepare varying levels of PODXL expression in the same cell line, LN229 (glioblastoma cell line) was used. LN229 hPODXL (LN229-PODXL) and LN229 hPODXL-knockout (LN229-PODXL-KO) cells were generated in previous studies [16]. LN229-PODXL was transfected with PODXL plasmid, including the full length of hPODXL. LN229-PODXL-KO cell was produced using CRISPR/Cas9 plasmids (Target ID: HS0000056763). NCI-H226 and human umbilical vein endothelial cells (HUVECs) were obtained from ATCC (Virginia, USA). LN229-PODXL and LN229-PODXL-KO cells were maintained in Dulbecco's Modified Eagle Medium supplemented with 10 % fetal bovine serum (FBS) and 2 mM penicillin-streptomycin-glutamine (PSG) solution (Merck KGaA, Darmstadt, Germany). NCI-H226 cells were maintained in RPMI-1640 medium (FUJIFILM Wako Pure Chemical Corporation, Osaka, Japan) supplemented with 10 % FBS and 2 mM PSG solution. HUVECs were maintained in EBM-2 BulletKit (Lonza, Basel, Switzerland). Peripheral blood mononuclear cells (PBMCs) were used to generate CAR-T cells. PBMCs were obtained from healthy volunteers. T cells were cultured in α-MEM (Merck KGaA) supplemented with 15 % FBS, 2 mM PSG (Thermo Fisher Scientific, MA, USA), 50 ng/mL ascorbic acid 2-phosphate (Merck KGaA), and 5 ng/mL recombinant human interleukin (rhIL)-7 (PeproTech, NJ, USA). For T cell

expansion, α-MEM was supplemented with 5 ng/mL rhIL-15 (PeproTech). All cell lines were cultured at 37 °C with 5 % CO2.

2.2. Fluorescence immunostaining (ICC/IF) of target cell lines

LN229-PODXL, LN229-wild type (WT), LN229-PODXL-KO, NCI-H226 cells, and HUVECs were fixed in 4 % PFA (Nacalai Tesque, Kyoto, Japan) for 15 min one day after seeding in 96 well plates (Greiner Bio-one, Kremsmünster, Austria) and then in 5 % BSA (Merck KGaA) in PBS for blocking. Primary antibody staining was performed using mouse IgG1 anti-PODXL antibody, PcMab-47 (1 mg/mL) [16]. Staining was performed for 1 h at a concentration of 1:100 dilution (10 μg/mL), followed by washing three times in PBS. Secondary antibody staining was performed using Goat Anti-Mouse IgG H&L Alexa Fluor 488 (Abcam, Cambridge, UK) at a
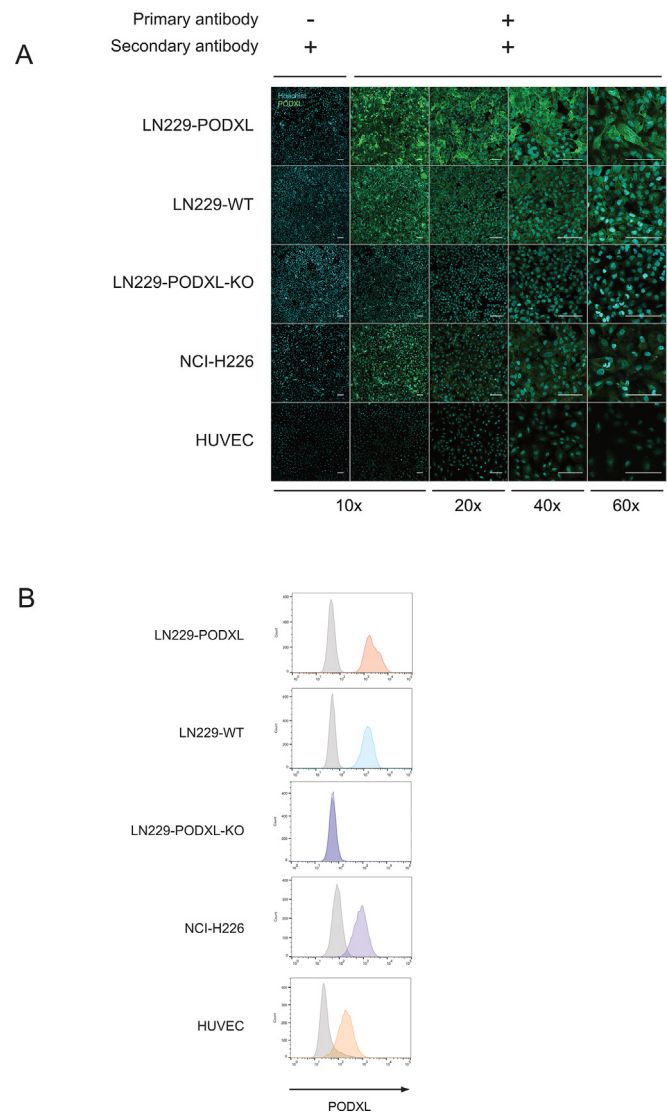

Fig. 1. Confocal microscopic images of tissue fluorescence immunostaining for PODXL expressed on cancer cells and primary cells, and flow cytometry plots. (A) Images of LN229 hPODXL, LN229-WT, LN229 PODXL-KO, NCI-H226 and HUVEC cells stained with anti-PODXL antibody, PcMab-47, and Goat Anti-Mouse IgG H&L (Alexa Fluor 488) as the secondary antibody. Images were taken at 10x, 20x, 40x and 60x magnification. Negative control was stained with secondary antibody only. The white bar is 100 μm. (B) Flow cytometry plots of cells stained with the same antibody combinations as in A. The top row is a merged image, and the expression levels of each PODXL are shown with the negative control of the secondary antibody only.

concentration of 1:200 dilution for 1 h, followed by washing and staining with Hoechst 33342 (Thermo Fisher Scientific) in PBS at 1:20000 diluted solution in PBS for 5 min, washed three times with PBS and photographed with a confocal microscope CellVoyager CQ1 (Yokogawa Electric Corporation, Tokyo, Japan) at 10x, 20x, 40x and 60x magnification, respectively. Negative controls were stained with secondary antibodies only.

2.3. FCM analysis

Flow cytometry was performed using LSR or FACS Aria II flow cytometers (BD, NJ, USA). Data were analyzed using FlowJo software (BD). Effector cells were stained with APC-Cy7 conjugated anti-CD3 antibody (BioLegend, CA, USA), APC-conjugated anti-CD4 antibody (BioLegend), FITC-conjugated anti-CD8 antibody (BioLegend), and BV421-conjugated anti-tEGFR antibody (BioLegend). Target cells were stained with mouse IgG1 anti-PODXL antibody, PcMab-47 as the primary antibody at a concentration of 1:1000 dilution (1 μg/mL).

2.4. Construction of retroviral vectors

ScFv antibodies PcMab-6 and PcMab-47, transmembrane domains, and intracellular domains were amplified by polymerase chain reaction (PCR) using KOD One PCR master mix-blue (TOYOBO, Osaka, Japan). The PCR conditions were 2 min of denaturation at 94 °C, followed by 35 cycles of 10 s of denaturation at 98 °C and 15 s of extension at 68 °C. The amplified genes were inserted into the pMY retroviral vector (Cell BioLabs, CA, USA) using NEBuilder HiFi Assembly (New England Biolabs, MA, USA).

2.5. Generation of PODXL CAR-T cells

RD18 cells were harvested two days before transfection in 10 cm dishes. CAR genes encoding retroviral vectors and the VSVG gene-encoding pMD2.G vector (Addgene, MA, USA) were transfected using DNA transfection reagents. To expand and activate T cells, PBMCs were stimulated with Dynabeads Human T-Activator CD3/CD28 (Thermo Fisher Scientific). On days 2 and 3, activated T cells were seeded into RetroNectin virus-coated 96-well plates for viral infection. The RetroNectin virus-coated 96-well plates were prepared by coating with 50 μg/mL RetroNectin (Takara Bio, Shiga,

Japan) and adding retrovirus, followed by centrifugation at 2000 g at 32 °C for 2 h.

2.6. Cytotoxicity assays

A non-radioactive cellular cytotoxicity assay kit (Techno Suzuta, Nagasaki, Japan) was used according to the manufacturer's instructions. Target cells (LN229-PODXL, LN229-PODXL-KO, NCI-H226, and HUVECs) were pulsed with BM-HT reagent at 37 °C for 15 min, washed three times, and seeded at 5×10^3 cells/well in 96-well plates. Co-culture supernatants (40 μl) were mixed with 160 μl of Eu solution, and time-resolved fluorescence was measured using a VICTOR Nivo multimode plate reader (PerkinElmer, MA, USA). These cells were cultured in α-MEM supplemented with 15 % FBS and 2 mM PSG at 37 °C with 5 % CO_2.

2.7. Time-lapse cytotoxicity assay using image analysis

The number of Et-hD positive cells was determined using the LIVE/DEAD Viability/Cytotoxicity Kit for mammalian cells (Thermo Fisher Scientific) and analyzed with the high content analysis system, CellPathfinder (Yokogawa Electric Corporation). The image recognition algorithm for identifying only dead target cells was configured with the following parameters: Method: T1, Detect Factor: 3.0, Nuclear Diameter: 20.0 μm, Division Mode: R1, Split Factor: 1.0, Min. Gray Offset: 10.0, Range: 45.0–340.0 μm^2. It was optimized to exclusively count the size of the target cells without including dead small effector cells in the count. Each of the four locations in the well was captured, and the mean and standard deviation were calculated using GraphPad Prism 8 (GraphPad Software, MA, USA). To reduce laser-induced injury, imaging was conducted using a microlens-enhanced Nipkow disk scanning (spinning disk) confocal microscope, CellVoyager CQ1 (Yokogawa Electric Corporation), with imaging performed every 5 min for 24 h.

2.8. Inflammatory cytokine production assays

BD Cytometric Bead Array Flex Set System (BD) was used to measure interferon-gamma (IFN-γ) levels. Supernatants were collected after 24 h of co-culture, centrifuged, and frozen until use. Approximately 1.0×10^6 resting CAR-T cells were maintained in α-MEM supplemented with 15 % FBS, 2 mM PSG, 50 ng/mL ascorbic
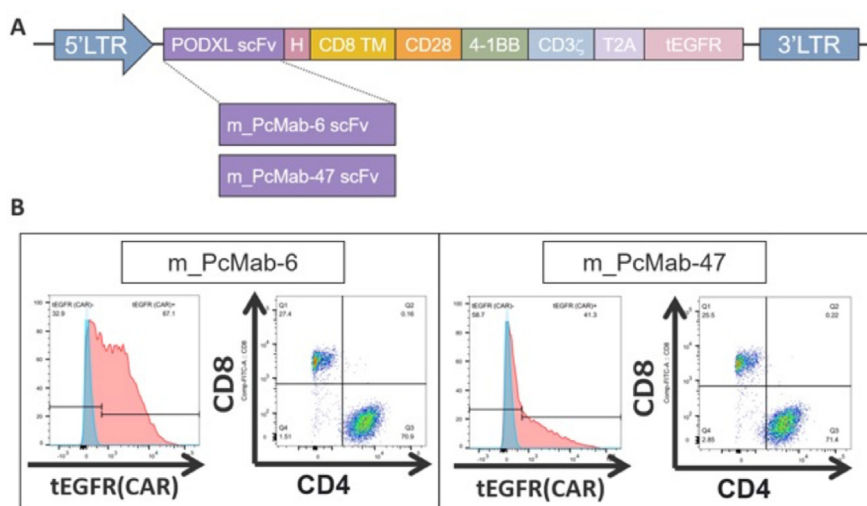

Fig. 2. Generation of m_PODXL CAR-T cells. (A) Schematic representation of retroviral vectors encoding m_PcMab-6 and m_PcMab-47 CARs. These vectors expressed tEGFR genes linked by T2A. (B) Flow cytometry plots of CD4, CD8, and tEGFR-positive CAR-T cells.

acid 2-phosphate, and 5 ng/mL rhIL-7, and cultured with 1.0×10^6 LN229-PODXL, LN229-PODXL-KO, NCI-H226 cells, or HUVECs.

2.9. In vivo animal models

Eight-week-old female NOD.Cg-*Prkdc*^{scid}*Il2rg*^{tm1Sug}/ShiJic (NOG) MHC-dKO (MHC class I- and class II-deficient) mice were purchased from CIEM (Kanagawa, Japan). In addition to the ability of NOG mice to engraft transplanted cells well, NOG-MHC-dKO mice were used with the aim of suppressing GVHD and extending the period of survival [24]. On day 0, 5.0×10^6 LN229-PODXL cells mixed with PBS and BD Matrigel Matrix (growth factor reduced) (BD) at a 3:5 ratio were subcutaneously injected. To evaluate mouse scFv CAR-T cells, 5.0×10^6 m_PcMab-6 CAR-positive T cells or CAR-negative T cells were intravenously injected on day 7. To evaluate human scFv CAR-T cells, 1.0×10^7 h_PcMab-6 CAR-positive T cells or CAR-negative T cells were intravenously injected on days 7, 9, and 11. CAR-T cells were prepared by retroviral transduction as described above. Dynabeads human T-activator CD3/CD28 (Thermo Fisher Scientific) was used to expand and activate T cells, and the cells were injected into mice on day 7. Tumor dimensions were measured with calipers, and tumor volume (V) was calculated using formula V = LW2/2, where L is the length (longest dimension) and W is the width (shortest dimension).

2.10. Statistical analysis

Data are expressed as mean ± standard deviation or mean ± standard error of the mean. All statistical analyses were performed using GraphPad Prism 8 (GraphPad Software) software. p-values were calculated using one-way or two-way analysis of variance (ANOVA) with Tukey's multiple comparison test and Student's t-test.

3. Results

3.1. Profiling of PODXL expression on target cells

To profile the cell surface expression of PODXL in target cells in detail, we performed immunofluorescence staining using the PcMab-47 antibody and FCM analysis. These analyses revealed that more PODXL molecules were overexpressed on the plasma membrane in LN229-PODXL cells than in WT cells. In PODXL-KO cells, the fluorescence intensity was equivalent to that of the secondary antibody-only negative control, confirming the absence of PODXL expression; NCI-H226 cells were larger but had higher fluorescence intensity than LN229-WT; HUVECs had the lowest fluorescence intensity but were confirmed to express PODXL; and LN229-PODXL cells had the highest fluorescence intensity of PODXL. (Fig. 1A and B).

3.2. Functional evaluation of mouse scFv CAR-T cells

Third-generation CARs containing CD28 and 4-1BB signal domains were generated from the scFv portions of m_PcMab-6 and m_PcMab-47, and retroviral vectors containing the CARs were introduced into human primary T cells (Fig. 2A). The transduction efficiency of each CAR gene was assessed using tEGFR expression levels. tEGFR-positive cells were 67.1 % in m_PcMab-6 with a CD4:CD8 ratio of 70.9:27.4. tEGFR-positive cells were 41.3 % in m_PcMab-47 with a CD4:CD8 ratio of 71.4:25.5. (Fig. 2B).

To evaluate whether m_PcMab-6 and m_PcMab-47 CAR-T cells were effective against PODXL-expressing cells, a cytotoxicity assay of CAR-T cells against PODXL-expressing cells was performed (Fig. 3A). Each CAR-T cell showed E: T ratio-dependent cytotoxicity against PODXL-expressing LN229-PODXL and NCI-H226 cells.

m_PcMab-47 CAR-T cells showed cytotoxicity against normal HUVECs, while m_PcMab-6 CAR-T cells did not (Fig. 3B).

Since the cytotoxicity of T cells is known to be influenced by the production of inflammatory cytokines, IFN-γ activity was evaluated 24 h after the co-culture of CAR-T cells with PODXL-expressing cells (Fig. 3C). Each CAR-T cell produced IFN-γ in response to LN229-PODXL and NCI-H226 cells expressing PODXL. m_PcMab-47 CAR-T cells produced IFN-γ in response to normal HUVECs, while m_PcMab-6 CAR-T cells did not produce significant levels of IFN-γ (Fig. 3D).

In addition to the short-term cytotoxicity evaluation, we conducted a long-term cytotoxicity assessment using a low ET ratio
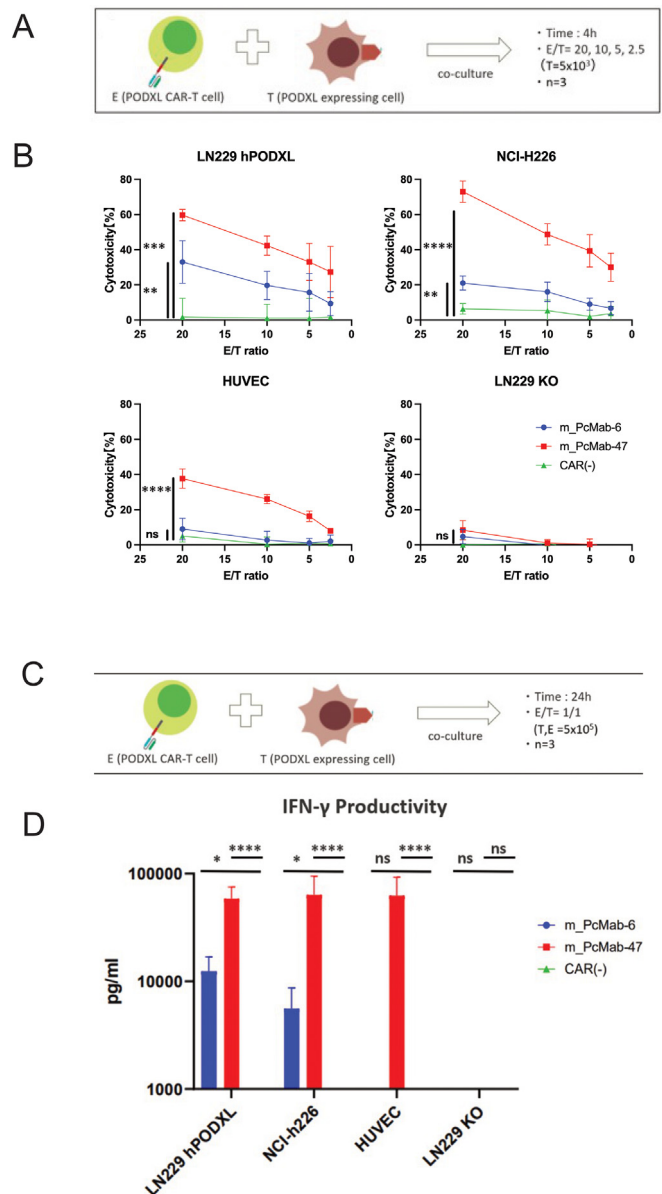

Fig. 3. *In vitro cytotoxicity assays and cytokine productionassays of m_CAR-T cells*. (A) Schematic representation of non-radioactive cytotoxicity assays. (B) *In vitro* cytotoxicity assays measured by non-radioactive cytotoxicity assay using LN229-PODXL, LN229-PODXL-KO, NCI-H226 cells, and HUVECs (n = 3). Data represent mean ± standard error from independent experiments. Statistical significance: *p < 0.05, **p < 0.01, ***p < 0.005, ****p < 0.001 by one-way ANOVA with Tukey's multiple comparison test. (C) Schematic representation of inflammatory cytokine production assays. (D) IFN-γ production by each CAR-T cell against PODXL-expressing cells (n = 3). Data represent mean ± standard error from independent experiments. Statistical significance: *p < 0.05, **p < 0.01, ***p < 0.005, ****p < 0.001 by one-way ANOVA with Tukey's multiple comparison test.

(E:T = 3:1) and an image analysis system. We used a Nipkow Disk Scanning confocal microscope to capture high-quality images of effector and target cells while minimizing light source toxicity to the cells. Images were taken every 5 min over a 24-h period (Fig. 4A and Supplementary Video). The data obtained was analyzed using image analysis, and the number of dead cells was measured using an algorithm that had been optimized in a preliminary study. The algorithm was adjusted so that only dead cells in the target cells were detected (Supplementary Fig. 1). In order to show that there is no toxic effect on cells due to long-term exposure to lasers or Et-hD under these experimental conditions, only the target cells were cultured under the same conditions on the same plate and photographed, but even after 24 h, almost no dead cells were observed (Fig. 4A and B right panel). The results of 24 h time laps tracking showed that LN229-PODXL was the most damaged, and even LN229-WT was damaged gradually over time. On the other hand, NCI-H226 showed almost no difference from LN229-KO, and the

number of dead cells in both cases leveled off at this low ET ratio (Fig. 4B).

Supplementary video related to this article can be found at https://doi.org/10.1016/j.reth.2024.12.010

To evaluate the anti-tumor activity of m_PcMab-6 CAR-T cells against PODXL-expressing cells, LN229-PODXL cells were subcutaneously injected into NOG-MHC-dKO mice (Fig. 5A). Seven days after the subcutaneous injection of tumors, m_PcMab-6 CAR-T cells and primary T cells were intravenously injected. Tumor diameters were measured over nine weeks, and tumor growth was suppressed in the m_PcMab-6 CAR-T cell-treated group for 14 days (Fig. 5B).

3.3. In vivo functional evaluation of human scFv CAR-T cells

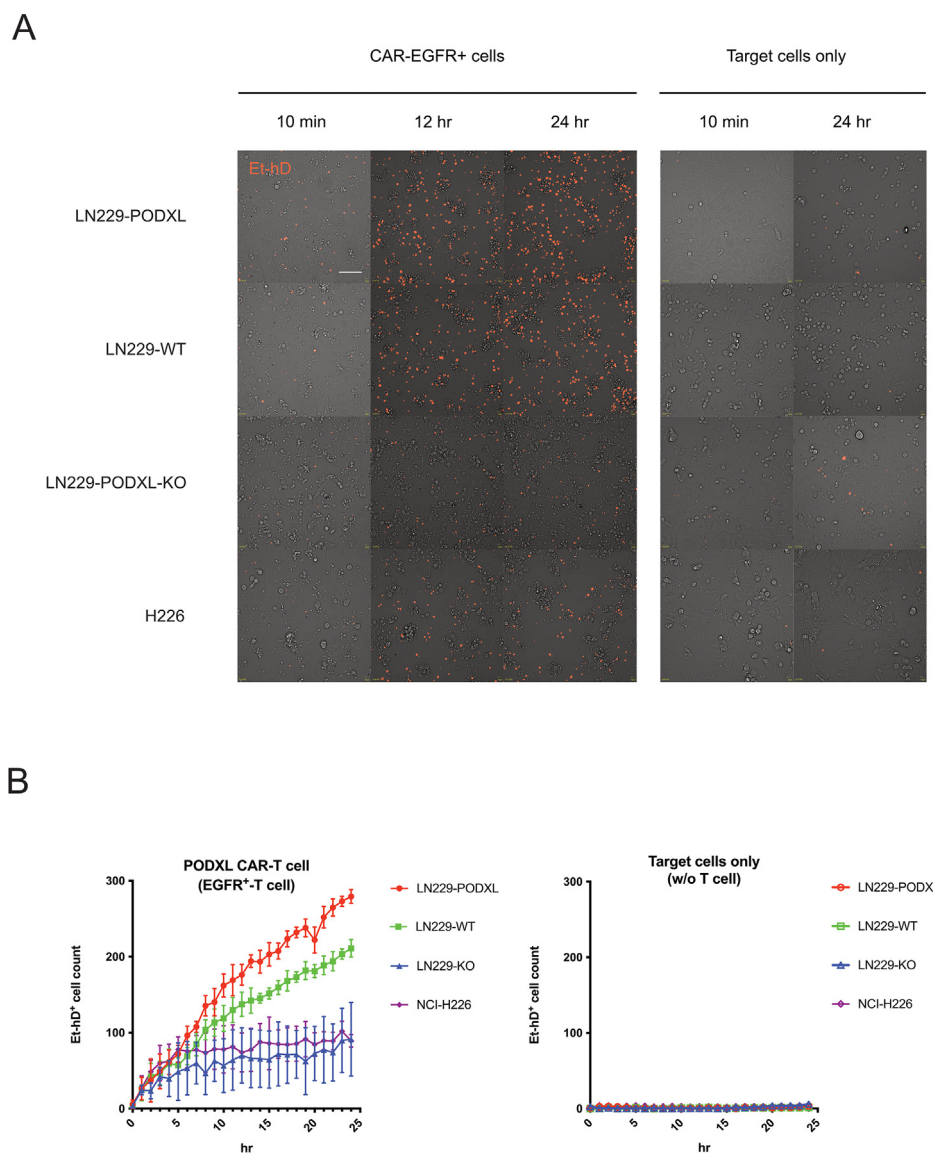Third-generation CAR was generated from the scFv portions of h_PcMab-6, and retroviral vectors containing the CAR were

Fig. 4. 24-h time-lapse tracking images of cytotoxicity using a Nipkow disk confocal microscope. (A) Dead cells (Et-hD-positive cells) are visible as red dots in the images. The images display the appearance of the target cells LN229-PODXL, LN229-WT, LN229-PODXL-KO, and H226 at 10 min, 12 h, and 24 h after staining with Et-hD. In the right panel, only the target cells were cultured under the same conditions to monitor the toxic effects of long-term exposure to lasers and Et-hD. The size of the white bar is 100 μm. (B) Comparison of the number of dead target cells in 24-h time-lapse imaging. The number of Et-hD-positive cells was extracted every 5 min using image recognition from the data shown in A and plotted over 24 h. Four fields of images were captured, and the average was plotted. The bar represents the standard deviation. The graph on the left shows the results of co-culturing target cells and CAR-T cells, while the graph on the right shows the results of culturing target cells alone under the same conditions.
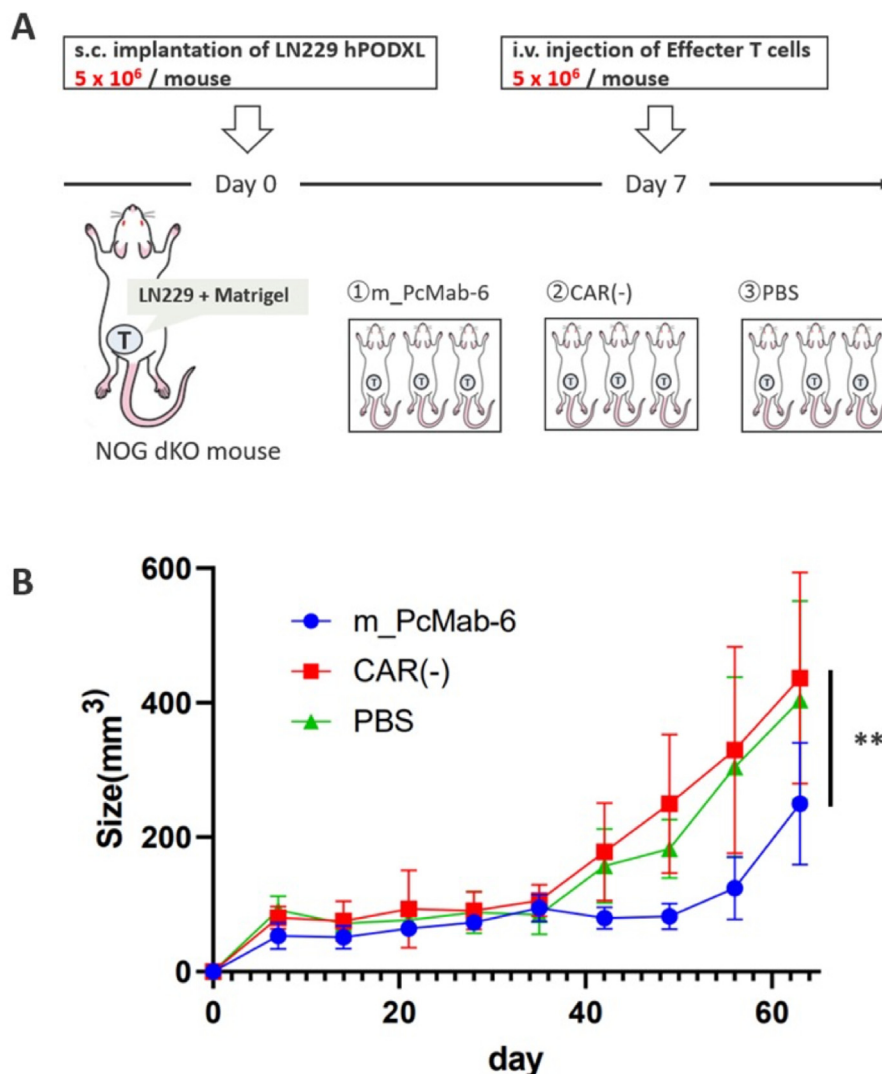
Fig. 5. m_CAR-T cells *in vivo* functional assessment assay. (A) LN229-PODXL cells and m_PcMab-6 CAR-T cells were injected subcutaneously and intravenously, respectively. (B) Tumor transits were measured in mice for nine weeks. *P < 0.05, **P < 0.01, ***P < 0.005, ****P < 0.001 by one-way ANOVA with Tukey's multiple comparison test.

introduced into primary T cells (Supplementary Fig. 2A) [23]. The transduction efficiency of each CAR gene was assessed using tEGFR fluorescence. h_PcMab-6 had 20.7 % tEGFR-positive cells with a CD4:CD8 ratio of 51.4:46.0. (Supplementary Fig. 2B).

As in the functional evaluation of Mouse scFv CAR-T cells, LN229-PODXL cells were inoculated subcutaneously into NOG-MHC-dKO mice to assess the anti-tumor activity of h_PcMab-6 CAR-T cells against PODXL-expressing cells (Fig. 6A). Seven, nine, and 11 days after tumor subcutaneous inoculation, h_PcMab-6 CAR-T and primary T cells were injected intravenously. Tumor transit was measured for nine weeks, and tumor progression was suppressed for 21 days in the h_PcMab-6 CAR-T cell-treated group (Fig. 6B).

4. Discussion

In this study, we developed novel CAR-T cells targeting PODXL using the CasMab technique, specifically recognizing cancer cells. These CAR-T cells demonstrated specific cytotoxicity and inflammatory cytokine production against PODXL-expressing cell lines *in vitro* and significantly suppressed tumor growth *in vivo* upon CAR-T cell administration. PODXL is known to promote tumor growth, invasion, and metastasis and is overexpressed in specific cancers. However, PODXL is also expressed in normal cells, raising

concerns about on-target off-tumor effects when used as a therapeutic target in CAR-T cell therapy.

In contrast, PcMab-6 CAR-T cells did not show cytotoxicity against normal HUVECs or significant production of inflammatory cytokines *in vitro*. Although *in vivo* safety evaluation and response to other PODXL-expressing normal cells must be observed in further studies, CasMab-based CAR-T cell therapy has the potential to improve the safety and specificity of targeting tumors. The scFv of CARs consists of complementarity-determining regions (CDRs) and framework (FR) regions responsible for antigen specificity and stability [25]. The CDR and FR sequences of scFvs vary among species. To address immunogenicity, it has been reported that the FR sequences are modified to human immunoglobulin sequences in the development of humanized CARs [26]. In this study, the researchers humanized a CAR that targets CD30. This antigen is already being used in clinical research, and interestingly, the cytotoxicity assays *in vitro* showed that CAR-T cells carrying the humanized CD30-CAR maintained a higher proportion of central memory cells (CCR7+ CD45RO + Tcm cells) than those that did not have the humanization. This result may be one of the mechanisms by which humanization enhances long-term persistence. Although the detailed mechanism of why Tcm is maintained at a high level has yet to be discovered, it is possible that continuous antigen
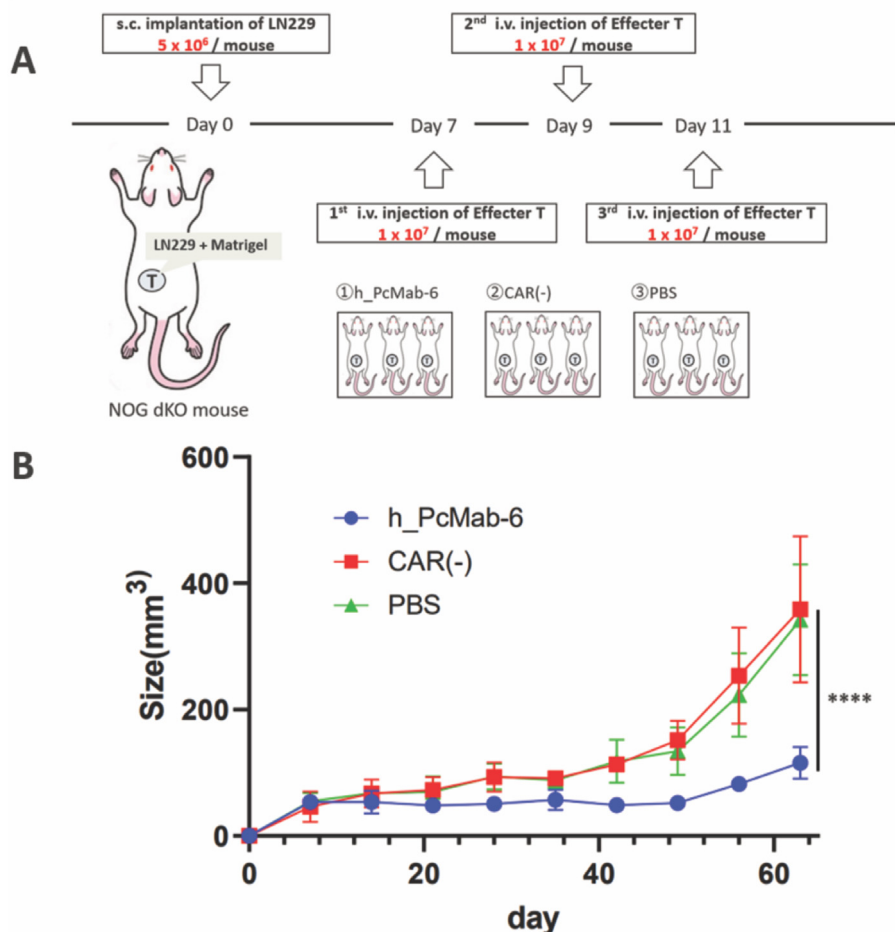
Fig. 6. *In vivo* functional evaluation assays of h_CAR-T cells. (A) Subcutaneous injection of LN229-PODXL cells and intravenous injection of h_PcMab-6 CAR-T cells. (B) Tumor diameters were measured for 9 weeks. Statistical significance: *p < 0.05, **p < 0.01, ***p < 0.005, ****p < 0.001 by one-way ANOVA with Tukey's multiple comparison test.

stimulation promotes the differentiation of Tcm into effector memory (Tem) cells. Similar results have also been reported in the clinical use of CD19-CAR [27], and it is predicted that the maintenance of the Tcm subset is important in the tumor microenvironment (TME), so it is likely that the humanization of CARs will also be clinically beneficial also in solid tumors. For this reason, we are also considering a detailed analysis of T cell subsets in the future for the PcMab-6 CAR. Our research also confirmed improved therapeutic efficacy by optimizing the CAR's CDR sequences to human codon sequences and modifying the FR sequences to match the human IgG1 antibody trastuzumab [28]. The impact of humanizing scFv sequences on therapeutic efficacy is an intriguing research topic requiring further investigation.

As reported in this study, the creation of CAR-T cells equipped with CasMab technology has the potential to turn PODXL, which is also expressed in normal cells, into a promising target for CAR-T cell therapy. This technology addresses the significant issue of on-target off-tumor effects in CAR-T cell therapy. In particular, the previous study has already shown that the PcMab-6 monoclonal antibody recognizes pancreatic ductal adenocarcinoma (PDAC) cell lines (MIA PaCa-2, Capan-2, PK-45H) but does not react with normal lymphatic endothelial cells (LEC). At the same time, the data has shown that PcMab-47, a non-CasMab, has high reactivity against both PDAC cell lines and LECs [23]. For this reason, we would like to give priority to examining the data on the PcMab-6 CAR-T cell targeting the PDAC cell line in the future, and we are expecting the

potential of PcMab-6 in pancreatic cancer. However, two concerns must be considered for clinical application. Firstly, the types of cell lines are limited at this stage, as the over-expression and deletion strains were created only for the LN229 cell line to control the expression level of PODXL. The cancer-specific modifications of PODXL molecules that were recognized by the PcMab-6 CAR may also differ in terms of their expression levels depending on the cancer cell line used. Additionally, when comparing the time-lapse data for LN229 and NCI-H226, it became apparent that the size of the target cells likely influenced their resistance to damage. Therefore, it is necessary to further confirm the cytotoxicity of CasMab to tumors and its safety to normal cells by using PODXL-expressing cancer cells and normal cells, which were not used in this study. We also plan to create transgenic mice expressing human PODXL and study the safety of PcMab-6 CAR-T cells. Secondly, the specific molecular mechanism of what is unique to cancer cells in the PODXL region recognized by PcMab-6 has not been clarified. In previous research, CasMab (LpMab-2) was developed to target Podoplanin (PDPN/Aggrus/T1α), and it has been reported that it recognizes aberrantly glycosylated Podoplanin [21]. Similarly, there is a high possibility of differences due to glycosylation, but further verification is required.

In this study, we developed CAR-T cells with CasMab technology that specifically recognizes tumors to reduce side effects in CAR-T cell therapy. CasMab-incorporated CAR-T cells demonstrated cytotoxicity and inflammatory cytokine production against PODXL-

expressing cell lines *in vitro* while not reacting to normal PODXL-expressing cells. *In vivo* mouse models also showed significant tumor growth suppression. Further, *in vivo* safety evaluations and observations of responses to other PODXL-expressing normal cells are necessary. However, CasMab-based CAR-T cell therapy may enhance safety and specificity for targeting tumors.

Ethics statement

This study was conducted in accordance with the tenets of the Declaration of Helsinki and was approved by the Institutional Ethical Board of Kyoto University. The Institutional Animal Research Committee approved animal experiments, and all experiments were performed in accordance with relevant guidelines and regulations. Healthy volunteers (from whom PBMCs were obtained) provided written informed consent.

Author contributions

Yuta Mishima: Data curation, Formal analysis, Investigation, Methodology, Visualization, Writing-original draft, Writing-review & editing, Funding acquisition.

Shintaro Okada: Data curation, Formal analysis, Visualization, Writing-original draft.

Akihiro Ishikawa: Data curation, Methodology, Investigation.

Wang Bo: Methodology, Investigation.

Masazumi Waseda: Data curation, Methodology, Investigation.

Mika K. Kaneko: Methodology, Investigation, Resources.

Yukinari Kato: Conceptualization, Methodology, Investigation, Resources, Funding acquisition.

Shin Kaneko: Conceptualization, Funding acquisition, Project administration, Resources, Supervision, Writing - review & editing.

Funding information

Declaration of competing interest

The authors declare the following financial interests/personal relationships which may be considered as potential competing interests: Shin Kaneko reports financial support was provided by Japan Agency for Medical Research and Development. Yukinari Kato reports financial support was provided by Japan Agency for Medical Research and Development. Yuta Mishima reports financial support was provided by Japan Society for the Promotion of Science. Yuta Mishima reports financial support was provided by Japan Science and Technology Agency. Yuta Mishima reports financial support was provided by Tsukuba Medical Laboratory of Education and Research. Shin Kaneko reports a relationship with Shinobi Therapeutics that includes: board membership, consulting or advisory, equity or stocks, funding grants, and travel reimbursement. Shin Kaneko reports a relationship with Takeda Pharmaceutical Company Limited that includes: consulting or advisory, funding grants, speaking and lecture fees, and travel reimbursement. Shin Kaneko reports a relationship with Astellas Pharma that includes: funding grants. Shin Kaneko reports a relationship with Panasonic Holdings Corporation that includes:

funding grants. If there are other authors, they declare that they have no known competing financial interests or personal relationships that could have appeared to influence the work reported in this paper.

Acknowledgments

Appendix A. Supplementary data

Supplementary data to this article can be found online at https://doi.org/10.1016/j.reth.2024.12.010.

References

[1] June CH, O'Connor RS, Kawalekar OU, Ghassemi S, Milone MC. CAR T cell immunotherapy for human cancer. Science 2018;359:1361–5. https://doi.org/10.1126/science.aar6711.

[2] Scarfò I, Maus MV. Current approaches to increase CAR T cell potency in solid tumors: targeting the tumor microenvironment. J Immunother Cancer 2017;5:28. https://doi.org/10.1186/s40425-017-0230-9.

[3] Schopperle WM, Kershaw DB, DeWolf WC. Human embryonal carcinoma tumor antigen, Gp200/GCTM-2, is podocalyxin. Biochem Biophys Res Commun 2003;300:285–90. https://doi.org/10.1016/s0006-291x(02)02844-9.

[4] Schopperle WM, DeWolf WC. The TRA-1-60 and TRA-1-81 human pluripotent stem cell markers are expressed on podocalyxin in embryonal carcinoma. Stem Cell 2007;25:723–30. https://doi.org/10.1634/stemcells.2005-0597.

[5] Hayatsu N, Kaneko MK, Mishima K, Nishikawa R, Matsutani M, Price JE, et al. Podocalyxin expression in malignant astrocytic tumors. Biochem Biophys Res Commun 2008;374:394–8. https://doi.org/10.1016/j.bbrc.2008.07.049.

[6] Toyoda H, Nagai Y, Kojima A, Kinoshita-Toyoda A. Podocalyxin as a major pluripotent marker and novel keratan sulfate proteoglycan in human embryonic and induced pluripotent stem cells. Glycoconj J 2017;34:817–23. https://doi.org/10.1007/s10719-017-9801-8.

[7] Bhattacharya B, Miura T, Brandenberger R, Mejido J, Luo Y, Yang AX, et al. Gene expression in human embryonic stem cell lines: unique molecular signature. Blood 2004;103:2956–64. https://doi.org/10.1182/blood-2003-09-3314.

[8] Zeng X, Miura T, Luo Y, Bhattacharya B, Condie B, Chen J, et al. Properties of pluripotent human embryonic stem cells BG01 and BG02. Stem Cell 2004;22:292–312. https://doi.org/10.1634/stemcells.22-3-292.

[9] Hayman MW, Przyborski SA. Proteomic identification of biomarkers expressed by human pluripotent stem cells. Biochem Biophys Res Commun 2004;316:918–23. https://doi.org/10.1016/j.bbrc.2004.02.141.

[10] Doyonnas R, Kershaw DB, Duhme C, Merkens H, Chelliah S, Graf T, et al. Anuria, omphalocele, and perinatal lethality in mice lacking the Cd34-related protein podocalyxin. J Exp Med 2001;194:13–28. https://doi.org/10.1084/jem.194.1.13.

[11] Flores-Téllez TNJ, Lopez TV, Garzón VRV, Villa-Treviño S. Co-expression of ezrin-CLIC5-podocalyxin is associated with migration and invasiveness in hepatocellular carcinoma. PLoS One 2015;10:e0131605. https://doi.org/10.1371/journal.pone.0131605.

[12] Snyder KA, Hughes MR, Hedberg B, Brandon J, Hernaez DC, Bergqvist P, et al. Podocalyxin enhances breast tumor growth and metastasis and is a target for monoclonal antibody therapy. Breast Cancer Res 2015;17:46. https://doi.org/10.1186/s13058-015-0562-7.

[13] Larsson A, Johansson ME, Wangefjord S, Gaber A, Nodin B, Kucharzewska P, et al. Overexpression of podocalyxin-like protein is an independent factor of poor prognosis in colorectal cancer. Br J Cancer 2011;105:666–72. https://doi.org/10.1038/bjc.2011.295.

[14] Hsu Y-H, Lin W-L, Hou Y-T, Pu Y-S, Shun C-T, Chen C-L, et al. Podocalyxin EBP50 ezrin molecular complex enhances the metastatic potential of renal cell carcinoma through recruiting Rac1 guanine nucleotide exchange factor ARHGEF7. Am J Pathol 2010;176:3050–61. https://doi.org/10.2353/ajpath.2010.090539.

[15] Lin C-W, Sun M-S, Wu H-C. Podocalyxin-like 1 is associated with tumor aggressiveness and metastatic gene expression in human oral squamous cell carcinoma. Int J Oncol 2014;45:710–8. https://doi.org/10.3892/ijo.2014.2427.

[16] Ogasawara S, Kaneko MK, Yamada S, Honma R, Nakamura T, Saidoh N, et al. PcMab-47: novel antihuman podocalyxin monoclonal antibody for immunohistochemistry. Monoclon Antibodies Immunodiagn Immunother 2017;36:50–6. https://doi.org/10.1089/mab.2017.0008.

[17] Itai S, Ohishi T, Kaneko MK, Yamada S, Abe S, Nakamura T, et al. Anti-podocalyxin antibody exerts antitumor effects via antibody-dependent cellular cytotoxicity in mouse xenograft models of oral squamous cell carcinoma. Oncotarget 2018;9:22480–97. https://doi.org/10.18632/oncotarget.25132.

[18] Itai S, Yamada S, Kaneko MK, Harada H, Kato Y. Immunohistochemical analysis using antipodocalyxin monoclonal antibody PcMab-47 demonstrates podocalyxin expression in oral squamous cell carcinomas. Monoclon Antibodies Immunodiagn Immunother 2017;36:220—3. https://doi.org/10.1089/mab.2017.0030.

[19] Yamada S, Itai S, Kaneko MK, Kato Y. Anti-podocalyxin monoclonal antibody 47-mG2a detects lung cancers by immunohistochemistry. Monoclon Antibodies Immunodiagn Immunother 2018;37:91—4. https://doi.org/10.1089/mab.2018.0002.

[20] Kaneko MK, Itai S, Yamada S, Kato Y. 47-mG2a: a mouse IgG2a-type of PcMab-47 useful for detecting podocalyxin in esophageal cancers by immunohistochemistry. Monoclon Antibodies Immunodiagn Immunother 2018;37:158—61. https://doi.org/10.1089/mab.2018.0003.

[21] Kato Y, Kaneko MK. A cancer-specific monoclonal antibody recognizes the aberrantly glycosylated podoplanin. Sci Rep 2014;4:5924. https://doi.org/10.1038/srep05924.

[22] Myers RM, Li Y, Leahy AB, Barrett DM, Teachey DT, Callahan C, et al. Humanized CD19-targeted chimeric antigen receptor (CAR) T cells in CAR-naive and CAR-exposed children and young adults with relapsed or refractory acute lymphoblastic leukemia. J Clin Oncol 2021;39:3044—55. https://doi.org/10.1200/jco.20.03458.

[23] Suzuki H, Ohishi T, Tanaka T, Kaneko MK, Kato Y. A cancer-specific monoclonal antibody against podocalyxin exerted antitumor activities in pancreatic cancer xenografts. Int J Mol Sci 2024;25:161. https://doi.org/10.3390/ijms25010161.

[24] Yaguchi T, Kobayashi A, Inozume T, Morii K, Nagumo H, Nishio H, et al. Human PBMC-transferred murine MHC class I/II-deficient NOG mice enable long-term evaluation of human immune responses. Cell Mol Immunol 2018;15:953—62. https://doi.org/10.1038/cmi.2017.106.

[25] Fujiwara K, Masutani M, Tachibana M, Okada N. Impact of scFv structure in chimeric antigen receptor on receptor expression efficiency and antigen recognition properties. Biochem Biophys Res Commun 2020;527:350—7. https://doi.org/10.1016/j.bbrc.2020.03.071.

[26] Guo J, He S, Zhu Y, Yu W, Yang D, Zhao X. Humanized CD30-targeted chimeric antigen receptor T cells exhibit potent preclinical activity against hodgkin's lymphoma cells. Front Cell Dev Biol 2022;9:775599. https://doi.org/10.3389/fcell.2021.775599.

[27] Zhao Y, Liu Z, Wang X, Wu H, Zhang J, Yang J, et al. Treatment with humanized selective CD19CAR-T cells shows efficacy in highly treated B-ALL patients who have relapsed after receiving murine-based CD19CAR-T therapies. Clin Cancer Res 2019;25:5595—607. https://doi.org/10.1158/1078-0432.ccr-19-0916.

[28] Ishikawa A, Waseda M, Ishii T, Kaneko MK, Kato Y, Kaneko S. Improved anti-solid tumor response by humanized anti-podoplanin chimeric antigen receptor transduced human cytotoxic T cells in an animal model. Gene Cell 2022;27:549—58. https://doi.org/10.1111/gtc.12972.